MECHANICS
МЕХАНИКА

UDC 539.3
https://doi.org/10.23947/2687-1653-2023-23-1-7-16

Original article

Construction of Forming Limit Diagram for Sheet Blanks from Aviation Aluminum Alloys

Sergey I Feoktistov, Ivan K Andrianov ✉
Komsomolsk-na-Amure State University, 27, Lenin Prospect, Komsomolsk-on-Amur, Russian Federation
✉ ivan_andrianov_90@mail.ru

Abstract

Introduction. The modern development of stamping aircraft manufacturing is inextricably linked with the assessment of the limiting capabilities of sheet blanks. However, the issue of defect-free forming of blanks made of aviation aluminum alloys is understudied. The importance of this issue is due to the fact that aluminum alloys are often used in the manufacture of thin-walled products for aviation purposes. During the implementation of shaping processes, various defects may appear, specifically, corrugation or unacceptable thinning. In this regard, the objective of the work was to construct a diagram of the limit deformations of the base aviation alloys and to conduct a comparative analysis of the limit deformation curves for these materials.

Materials and Methods. Logarithmic deformations with the property of additivity were used to account for large deformations. The construction of the diagram of the limit deformations was carried out in the formulation of the deformation theory of plasticity. The issue of constructing a diagram of limit deformations was considered on the basis of the positivity criterion of the loading force derivative. In the area of negative values of the smallest major deformations, the Hill criterion was used to construct the limit deformation curve, and in the area of positive values of the smallest major logarithmic deformations, the Swift criterion was used. When constructing the limit deformation diagram, a power approximation of the hardening rule was used.

Results. The curves of limiting deformations for the following aviation alloys were obtained: AMg6, D16AT, AMg2M, 1201-T, AMcM. According to the comparative analysis of the areas of safe forming, the values of deformations of the beginning of necking and their influence on the change in the position of the curve of the limiting deformation of blanks were compared: the greater the deformation of the neck formation, the higher the position of the curve of the limiting deformations. The concept of the Keeler's limit deformation diagram was described. Approaches to the construction of the Hill-Swift criteria used on the basis of the results of tensile testing of sheet specimens were presented.

Discussion and Conclusions. Based on the constructed curves of limiting deformations for aviation alloys, AMg-6, D16AT, AMg2M, 1201-T, AMcM, the following has been found. AMg2M alloy has the largest area of safe forming, 1201-T alloy has the smallest one. That is explained by the difference in relative deformations of the beginning of neck formation. The conducted research made it possible to evaluate the possibilities of defect-free forming of thin-walled blanks made of basic aviation aluminum alloys. The use of the constructed diagrams of limiting deformation will provide predicting the appearance of breaks in the process of forming sheet blanks.

Keywords: sheet stamping, forming limit diagram, logarithmic strains, Hill-Swift diagram.

Acknowledgements. Appreciation is expressed to the “Council for grants of the President of the Russian Federation for state support of young Russian scientists and for state support of leading scientific schools of the Russian Federation” for financial support of the research under scholarship project SP-2200.2022.5 “Development of models and algorithms for calculating the plastic shaping of blanks for stamping production”.

For citation. Feoktistov SI, Andrianov IK. Construction of Forming Limit Diagram for Sheet Blanks from Aviation Aluminum Alloys. *Advanced Engineering Research (Rostov-on-Don).* 2023;23(1):7–16. https://doi.org/10.23947/2687-1653-2023-23-1-7-16

Научная статья

Построение диаграммы предельных деформаций формоизменения листовых заготовок из авиационных алюминиевых сплавов

С.И. Феоктистов, И.К. Андрианов ✉

Комсомольский-на-Амуре государственный университет, Российская Федерация, г. Комсомольск-на-Амуре, пр. Ленина, 27

✉ ivan_andrianov_90@mail.ru

Аннотация

Введение. Современное развитие штамповочного авиастроительного производства неразрывно связано с оценкой предельных возможностей листовых заготовок. Однако малоизученным является вопрос бездефектного формоизменения заготовок из авиационных алюминиевых сплавов. Важность данного вопроса связана с тем, что алюминиевые сплавы достаточно часто используются при изготовлении тонкостенных изделий авиационного назначения. При реализации процессов формообразования возможно появление различных дефектов — гофрообразования или недопустимого утонения. В связи с этим целью работы являлось построение диаграммы предельных деформаций основных авиационных сплавов и проведение сравнительного анализа кривых предельного деформирования для данных материалов.

Материалы и методы. Для учета больших деформаций были использованы логарифмические деформации, обладающие свойством аддитивности. Построение диаграммы предельных деформаций формоизменения проводилось в постановке деформационной теории пластичности. Вопрос построения диаграммы предельных деформаций рассмотрен на основании критерия положительности производной силы нагружения. В области отрицательных значений наименьших главных деформаций для построения кривой предельного деформирования использовался критерий Хилла, а в зоне положительных значений главных наименьших логарифмических деформаций — критерий Свифта. При построении диаграммы предельного деформирования использовалась степенная аппроксимация закона упрочнения.

Результаты исследования. Получены кривые предельных деформаций для авиационных сплавов: АМг-6, Д16АТ, АМг2М, 1201-Т, АМцМ. Согласно проведенному сравнительному анализу областей безопасного формоизменения, сопоставлены значения деформаций начала шейкообразования и их влияние на изменение положения кривой предельного деформирования заготовок: чем больше деформация шейкообразования, тем выше положение кривой предельных деформаций. Описана концепция диаграммы предельных деформаций Килера. Представлены подходы к построению критериев Хилла и Свифта, используемых по результатам испытания листовых образцов на разрыв.

Обсуждение и заключения. На основании построенных кривых предельных деформаций для авиационных сплавов АМг-6, Д16АТ, АМг2М, 1201-Т, АМцМ выяснили, что наибольшую область безопасного формоизменения имеет сплав АМг2М, наименьшую — сплав 1201-Т, что объясняется отличием относительных деформаций начала шейкообразования. Проведенное исследование позволило оценить возможности бездефектного формоизменения тонкостенных заготовок из основных авиационных алюминиевых сплавов. Применение построенных диаграмм предельного деформирования позволит прогнозировать появление разрывов в процессе формообразования листовых заготовок.

Ключевые слова: листовая штамповка, диаграмма предельных деформаций, логарифмические деформации, диаграмма Хилла-Свифта.

Благодарности. Авторы выражают благодарность «Совету по грантам Президента Российской Федерации для государственной поддержки молодых российских учёных и по государственной поддержке ведущих научных школ Российской Федерации» за финансовую поддержку для проведения исследования в рамках стипендии по проекту СП-2200.2022.5 «Разработка моделей и алгоритмов расчёта пластического формообразования заготовок штамповочного производства».

Для цитирования: Феоктистов С.И., Андрианов И.К. Построение диаграммы предельных деформаций формоизменения листовых заготовок из авиационных алюминиевых сплавов. *Advanced Engineering Research (Rostov-on-Don).* 2023;23(1):7–16. https://doi.org/10.23947/2687-1653-2023-23-1-7-16

Introduction. Modern development of the aviation production is inextricably linked with the study of sheet stamping processes. One of the key problems in the task of shaping is the defect prediction, in particular, thinning, ruptures, corrugation. These issues are related to the assessment of the limits of the blank. By forming limit of a sheet blank, we will mean the ability of the material to deform to the required geometry without necking or destruction.

To date, the problem of predicting defects of sheet blanks in the stamping process is solved using the following methods:

– empirical, based on mechanical tests for simple stretching of metal samples, thin sheets and tapes, bending tests, as well as pipe testing methods for flaring and broaching;

– theoretical and empirical, which are based on the use and dissemination of the test results of samples for uniaxial tension to other schemes of deformation of blanks;

– theoretical, which are based on the use of criteria for limit deformation, specifically, in the manufacture of thin-walled products. The founders of these methods were J. Sachs, R. Hill, A. D. Tomlenov, V. D. Golovlev, G. D. Del, Z. Marciniak, A. D. Matveev, J. D. Lubahn [1–20].

It should be noted that the disadvantage of empirical and theoretical-empirical methods is the limited use of the results.

The most important step in solving the problem of predicting defects of thin-walled products was the development of the concept of the forming limit diagram (FLD) proposed by S. P. Keeler [16–20], which today is generally accepted in solving sheet stamping problems. FLD diagrams are widely used in AUTOFORM and PAM-STAMP 2G CAE software systems.

Experimental methods for constructing deformation diagrams are based on the test methodology presented in the works of Marciniak and Nakazima. It should also be noted that the issues of plastic destruction of sheet blanks were considered in [17–19]. In the last decade, interest in the construction of FLD diagrams has grown significantly. Most foreign studies are aimed at experimental construction of diagrams for specific materials, as well as numerical modeling of shape-changing processes using finite element methods [20–30]. Theoretical aspects of the construction of DFD diagrams and deformation diagrams of the third kind are presented in [31, 32].

It is important to note that the diagram of limit deformations provides estimating the beginning of neck formation, which ends with the destruction of the sample in the process of deformation. The FLD diagram binds the values of the main logarithmic deformations acting in the plane of the sheet. Forming limit diagrams enable not only to predict the destruction of the blank, but also to assess the presence of other defects, in particular, wrinkling, thinning, which, in turn, reduce the quality of the stamped part. The main zones of the FLD diagram are the zones of destruction, possible ruptures, safe forming, probable formation of folds, and wrinkling (Fig. 1) [31].

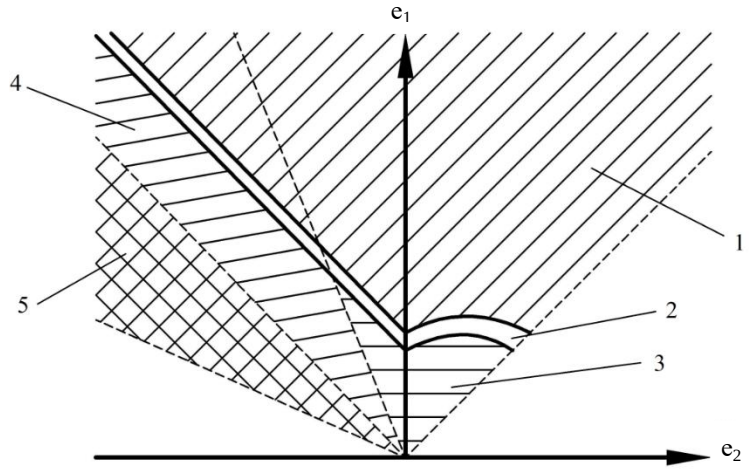

Fig. 1. Forming limit diagram: 1 — zone of destruction; 2 — zone of possible ruptures; 3 — zone of safe forming; 4 — zone of probable formation of folds; 5 — zone of wrinkling [31]

Materials and Methods. When describing the processes of forming thin-walled blanks, the moment of transition to the plasticity stage is determined in accordance with the Huber-von Mises criterion [33]:

$$\sigma_i = \sqrt{\sigma_1^2 + \sigma_2^2 - \sigma_1\sigma_2} = \sigma_\text{T},$$

where σ_1, σ_2 — primary true stresses, at $\sigma_3 = 0$ due to the light gauge of the blank; σ_i — intensity of true stresses; σ_T — yield strength.

According to the deformation theory of plasticity, the relationship between the intensity of stresses and the intensity of logarithmic deformations is defined as:

$$\left.\begin{aligned} e_1 &= \frac{e_i}{\sigma_i}\left(\sigma_1 - \frac{1}{2}\sigma_2\right), \\ e_2 &= \frac{e_i}{\sigma_i}\left(\sigma_2 - \frac{1}{2}\sigma_1\right), \end{aligned}\right\} \quad (1)$$

where $e_1, e_2,$ — principal deformations.

Since in sheet stamping tasks, the shaping processes can occur in several transitions, therefore, large deformations are considered. The use of relative deformations is unacceptable. In this regard, the deformed state in (1) is presented in true logarithmic deformations.

Intensity of the principal deformations:

$$e_i = \frac{2}{\sqrt{3}}\sqrt{e_1^2 + e_2^2 + e_1 e_2}.$$

The ratio of the principal deformations and the primary true stresses:

$$\alpha = \frac{e_2}{e_1}, \beta = \frac{\sigma_2}{\sigma_1}. \quad (2)$$

Based on ratio (1) and (2), the relationship between α and β is determined by:

$$\beta = \frac{2\alpha+1}{2+\alpha}. \quad (3)$$

According to expression (2), the Huber-von Mises criterion has the form:

$$\sigma_i = \sigma_1\sqrt{1 - \beta + \beta^2} = \sigma_\text{T},$$

and the intensity of deformations:

$$e_i = \frac{2}{\sqrt{3}} e_1 \sqrt{1 + \alpha + \alpha^2}. \quad (4)$$

To assess the onset of necking, the criterion of positivity of the derivative of the loading force is currently used, the founders of which were G. Sachs and J. D. Lubahn [17]. According to the described criterion, the deformation of the sample is stable with a positive increment of the tensile force. The moment of unstable deformation with subsequent stretching starts at $\Delta P = 0$ and continues at $\Delta P < 0$ (Fig. 2).

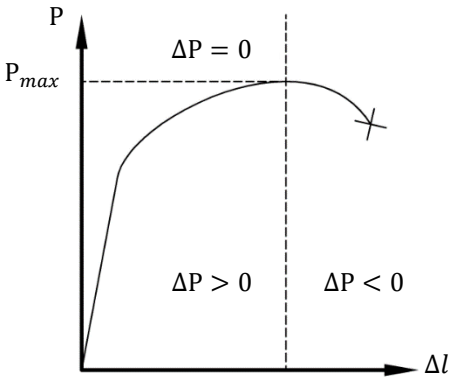

Fig. 2. Indicator diagram of uniaxial tension of the sample [33]

The deformation diagram of aluminum alloys obtained by the results of the uniaxial tensile test is approximated by a power function in the theoretical analysis of the diagrams of the limit deformations of the shape change [18, 19, 31, 32]:

$$\sigma_S = Ae^n \text{ или } \sigma_i = Ae_i^n,$$

where $\sigma_S = P/F$ — true stress; P — tensile force; F— current cross-sectional area of the sample; $e = \ln(1 + \Delta l/l_0)$, while A and n — coefficients of the power approximation.

Using the criterion of positivity of the derivative of the loading force and the power approximation of the deformation diagram of the third kind, it is possible to obtain a relationship between the limit deformation of the sample at the time of the occurrence of the diffuse neck and the power approximation coefficient n under condition $\Delta P = 0$ (Fig. 3) [32]:

$$e_{\text{ш}} = e_{i\text{ш}} = n. \quad (5)$$

It is significant that relation (1) is performed using logarithmic deformations. In case of using relative deformations, only approximate equality is possible.

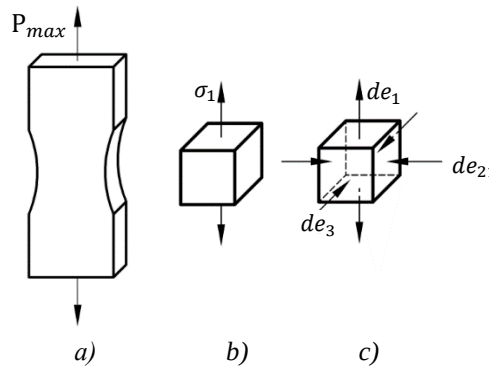

Fig. 3. Occurrence of a diffuse neck under uniaxial tension of a flat sample:
a — sample; *b* — stress state; *c* — deformed state [33]

Consider the stress state of a plate to which two tensile forces are applied at the edges, i.e., the blank experiences biaxial tension (Fig. 4).

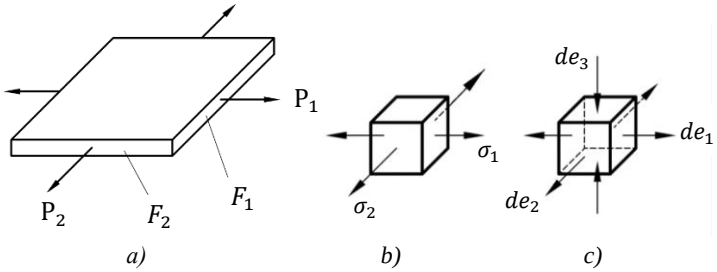

Fig. 4. Stress-strain state of the plate under biaxial tension: *a* — plate; *b* — stress state; *c* — deformed state [33]

Using the criterion of positivity of the derivative of the loading force, we determine the deformation limit value $e_{iш}$ at the moment when forces P_1 or P_2 are maximum. For the case when $F_2/F_1 = \text{const}$, $P_2/P_1 = \text{const}$, at the moment of maximum tensile forces $dP_1 = dP_2 = 0$. H. W. Swift [19] proposed the relation for the limit deformation:

$$e_{iш} = 4n\frac{(1-\beta+\beta^2)^{3/2}}{4-3\beta-3\beta^2+4\beta^3}.$$

According to expressions (2)–(4), the relation for describing the curve of limit deformations at various exponents of power approximation in the hardening zone has the form:

$$4(e_1-n)(e_2+2e_1)^3-3(e_1-2n)(e_1+2e_2)(e_2+2e_1)^2- \\ -3(e_1+2n)(e_2+2e_1)(e_1+2e_2)^2+2(2e_1+n)(e_1+2e_2)^3=0. \quad (6)$$

It is known from the experimental and theoretical studies that after the occurrence of a diffuse neck, plastic deformation of the sample continues. Thereafter, a localized neck may occur, which differs from the diffuse one not only in size, but also in that its occurrence and development are carried out under conditions of flat deformation with intensive thinning of the sample.

According to R. Hill [20], the limit deformation criterion is determined by the moment of formation of the local neck, at which the increment of the total force is zero. In this case, the relation for the limit deformation is determined by the expression:

$$e_{iш} = 2n\frac{(1-\beta+\beta^2)^{1/2}}{1+\beta}. \quad (7)$$

Taking into account expressions (2), (4), expression (7) for constructing a limit deformation diagram according to the Hill criterion has the form:

$$e_1+e_2-n=0. \quad (8)$$

It should also be noted that the described approach is consistent with the finite element method, which has been widely used to construct FLD diagrams of various materials in recent years [21–29].

Research Results. In practice, we will construct the FLD diagram using two criteria [31], namely: the Hill criterion, which is used for $e_2 \le 0$ according to (8); the Swift criterion, which is used for $e_2 \ge 0$ according to (6). Let us consider the application of these relations to construct the curve of the limit deformations of aluminum alloys widely used in the aviation industry at known values of deformation of necking: $\varepsilon_ш = 0.18$ (AMg6), $\varepsilon_ш = 0.16$ (D16AT), $\varepsilon_ш = 0.2$ (AMg2M), $\varepsilon_ш = 0.06$ (1201-T), $\varepsilon_ш = 0.1$ (AMcM) [34].

Determining $e_ш$ from formula $e_ш = \ln(1+\varepsilon_ш)$ and using expression (5), we obtain the value of the strain-hardening indices: $n = 0.17$ (AMg6), $n = 0.15$ (D16AT), $n = 0.18$ (AMg2M), $n = 0.06$ (1201-T), $n = 0.09$ (AMcM). Then, the Hill-Swift diagram, according to (6), (8), will take the form shown in Figure 5.

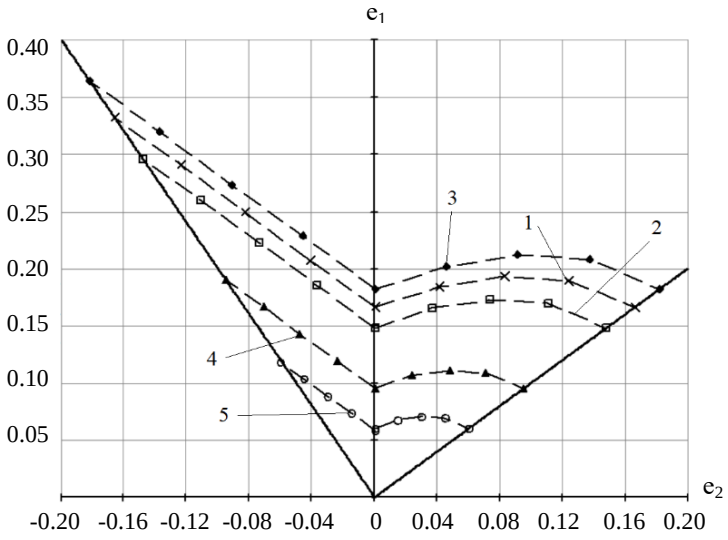

Fig. 5. FLD-Hill-Swift diagrams for various aviation alloys: 1 — AMg6 alloy; 2 — D16AT alloy; 3 — AMg2M alloy; 4 — 1201-T alloy; 5 — AMcM alloy

Discussion and Conclusions. According to the constructed curves of limit deformations, AMg2M alloy has the largest area of safe forming of the five alloys studied, 1201-T alloy has the smallest one. That is due to differences in the deformation properties of materials, specifically, the difference in the deformations of the necking onset. In AMg2M alloy, the relative deformation of the beginning of neck formation is 20 %, and in 1201-T alloy — 6 %.

Thus, on the basis of data on the hardening curves, power approximation and deformation of necking for aviation aluminum alloys AMg6, D16AT, AMg2M, 1201-T, AMcM, curves of limit deformations of forming have been constructed, providing for the determination of the zone of safe deformation of sheet blanks. The study results are of practical importance in solving sheet stamping problems for these materials to predict unacceptable thinning, raptures, and wrinkling of thin-walled blanks.

References

1. Narayanasamy R, Narayanan S. Forming Limit Diagram for Interstitial Free Steels Supplied by Ford India Motors. *Materials and Design*. 2007;28(1):16–35. https://doi.org/10.1016/j.matdes.2005.06.021

2. Krishnan E, Narayanan S, Narayanasamy R. Modelling of Forming Limit Diagram of Perforated Commercial Pure Aluminium Sheets Using Artificial Neural Network. *Computational Materials Science*. 2010;47:1072–1078. https://doi.org/10.1016/j.commatsci.2009.12.016

3. Li B, Nye TJ, Wu PD. Predicting the Forming Limit Diagram of AA 5182-O. *Journal of Strain Analysis for Engineering Design*. 2010;45(4):255–273. https://doi.org/10.1243/03093247JSA608

4. Hong Wei Liu, Peng Zhang. Forming Limit Diagram of Stainless Steel-Aluminum Alloy Clad. *Advanced Materials Research*. 2011;152–153:541–544. https://doi.org/10.4028/www.scientific.net/AMR.152-153.541

5. Chamos AN, Labeas GN, Setsika D. Tensile Behavior and Formability Evaluation of Titanium-40 Material Based on the Forming Limit Diagram Approach. *Journal of Materials Engineering and Performance*. 2013;22(8):2253–2260. https://doi.org/10.1007/s11665-013-0495-1

6. Feoktistov SI, Kyaw Zayar Soe. Method for Construction of Forming Limit Diagram by Using Reference Mechanical Characteristics of the Metal. *Materials Science Forum*. 2019;945:833–838. https://doi.org/10.4028/www.scientific.net/MSF.945.833

7. Zhiying Sun, Hong Zhuang. Experimental Study on Forming Limit Diagram Obtained by Bulging Uniformly in Thickness Direction. *The International Journal of Advanced Manufacturing Technology*. 2019;104:967–977. https://doi.org/10.1007/s00170-019-03887-9

8. Min-A Woo, Woo-Jin Song, Beom-Soo Kang, et al. Acquisition and Evaluation of Theoretical Forming Limit Diagram of Al 6061-T6 in Electrohydraulic Forming Process. *Metals*. 2019;9:401. https://doi.org/10.3390/met9040401

9. Glushchenkov VA, Chernikov DG, Tiabashvili AT. Method of Dynamic Test of Sheet Materials with Pulse Magnetic Loading. *Actual Problems in Machine Building*. 2017;4:94–99.

10. Davidenko M, Davidenko A, Matveev V, et al. Definition of the Limit Strain Fiber Concrete Deformations Based on the Energy Dependences of Concrete Deformation Diagrams. *Nauchnyi vestnik GOU LNR LGAU*. 2020;8(3):214–219.

11. Mamutov VS, Mamutov AV, Arsentyeva KS, et al. Ehksperimental'no-raschetnaya diagramma predel'nykh deformatsii dlya proektirovaniya ehlektrogidroimpul'snoi shtampovki. *Modern Mechanical Engineering. Science and Education*. 2021;10:611–622. (In Russ.).

12. Keller IE, Petukhov DS, Kazantsev AV, et al. The Limit Diagram under Hot Sheet Metal Forming. A Review of Constitutive Models of Material, Viscous Failure Criteria and Standard Tests. *Journal of Samara State Technical University, Ser. Physical and Mathematical Sciences*. 2018;22:447–486. http://doi.org/10.14498/vsgtu1608

13. Bezgodov IM, Dmitrenko EN. Improvement of Curvilinear Diagrams of Concrete Deformation. *Industrial and Civil Engineering*. 2019;8:99–104. https://doi.org/10.33622/0869-7019.2019.08.99-104

14. Eryshev VA. Numerical Methods of Strengthening Strength of Reinforced Concrete Elements on a Nonlinear Deformation Model with the Use of Diagrams of Material Breaking. *Bulletin NGIEI*. 2018;85(6):17–26.

15. Izosimova SV. Issledovanie vliyaniya formy zagotovki na tochnost' postroeniya diagrammy predel'nykh deformatsii. *Molodezhnyi nauchno-tekhnicheskii vestnik*. 2013;10:3. (In Russ.).

16. Feoktistov SI, Kyaw Zayar Soe. Determination of Technological Possibilities of Titanium and Aluminum Alloys at Distribution. *Scholarly Notes of KNASTU*. 2019;37(1):4–9.

17. Feoktistov SI, Zho Zayar So. Determination of the Limiting Expanding Ratio by FLD-Diagrams. *Forging and Stamping Production. Material Working by Pressure*. 2019;9:3–7.

18. Feoktistov SI, Zho Zayar So. Determination of the Limiting Drawing Ratio of Titanium and Aluminum Alloys by FLD-Diagrams. *Forging and Stamping Production. Material Working by Pressure*. 2019;5:27–34.

19. Swift HW. Plastic Instability under Plane Stress. *Journal of the Mechanical and Physics of Solids*. 1952;1:1–18. https://doi.org/10.1016/0022-5096(52)90002-1

20. Hill R. On Discontinuous Plastic States with Special Reference to Localized Necking in Thin Sheet. *Journal of the Mechanics and Physics of Solids*. 1952;1:19–30. https://doi.org/10.1016/0022-5096(52)90003-3

21. Petroušek P, Kočiško R, Kvackaj T, et al. Formability Evaluation of Aluminium Alloys by FLD Diagrams. *Acta Physica Polonica A*. 2017;131:1344–1347. http://dx.doi.org/10.12693/APhysPolA.131.1344

22. Lisiecka-Graca P, Kwiecień M, Madej Ł, et al. Application of the DIC System to Build a Forming Limit Diagram (FLD) of Multilayer Materials. *Key Engineering Materials*. 2022;926:963–969. http://dx.doi.org/10.4028/p-s33fqx

23. Rubešová K, Rund M, Rzepa S, et al. Determining Forming Limit Diagrams Using Sub-Sized Specimen Geometry and Comparing FLD Evaluation Methods. *Metals*. 2021;11:484. http://dx.doi.org/10.3390/met11030484

24. Marrapu B. Effect of Localization Criteria and Yield Criteria in Predicting the Forming Limit Diagram (FLD) of DP590 Steel Sheets. *Advances in Materials and Processing Technologies*. 2021;8(1):1739–1752. https://doi.org/10.1080/2374068X.2021.1874710

25. Guangyong Sun, Wenwu Zhang, Zhen Wang, et al. A Novel Specimen Design to Establish the Forming Limit Diagram (FLD) for GFRP through Stamping Test. *Applied Science and Manufacturing*. 2020;130:105737. http://dx.doi.org/10.1016/j.compositesa.2019.105737

26. Panahizadeh V, Hoseinpour M, Gholamzadeh E, et al. Theoretical and Experimental Study of FLDs of AA5083 Sheet and Investigation of Advanced Anisotropic Yield Criteria Coefficients. *Journal of the Brazilian Society of Mechanical Sciences and Engineering*. 2022;44:356. http://dx.doi.org/10.1007/s40430-022-03600-0

27. Godage O, Kakandikar G. Numerical and Analytical Investigation of Forming Limit Diagram of SS316L Foil. *International Journal for Research in Applied Science and Engineering Technology*. 2022;10:1544–1549. https://doi.org/10.22214/ijraset.2022.40899

28. Mahalle G, Takalkar P, Kotkunde N, et al. Strain and Stress-Based Forming Limit Diagrams for Inconel 718 Alloy. In book: *NUMISHEET 2022, Proc. 12th Int. Conference and Workshop on Numerical Simulation of 3D Sheet Metal Forming Processes.* 2022;1:549–556. http://dx.doi.org/10.1007/978-3-031-06212-4_50

29. Takalkar AS, Koteswara Rao JM, Mailan Chinnapandi LB. Numerical Simulation for Predicting Failure in Deep Drawing Process Using Forming Limit Diagram (FLD). *International Journal of Advances in Mechanical and Civil Engineering*. 2015;2:11–15.

30. Sekhara Reddy AC, Sandeep B, Sandeep Kumar J, et al. Experimental Determination of Anisotropic Properties and Evaluation of FLD for Sheet Metal Operations. *Advances in Science and Technology*. 2021;106:39–45. http://dx.doi.org/10.4028/www.scientific.net/AST.106.39

31. Lonardi C, Corallo L, Verleysen P. Prediction of Forming Limit Diagram Using the Marciniak-Kuczynski Method for Ti-6Al-4V Using Different Material Models. *Key Engineering Materials*. 2022;926:885–896. http://dx.doi.org/10.4028/p-10z13b

32. Paul SK. Theoretical Analysis of Strain- and Stress-Based Forming Limit Diagrams. *Strain Analysis*. 2013;48(3):177–188. http://dx.doi.org/10.1177/0309324712468524

33. Chumadin AS. *Teoriya i raschety protsessov listovoi shtampovki (dlya inzhenerov)*. Moscow: Ehksservis “VIP”; 2014. 216 p. (In Russ.).

34. Andrianov IK, Tun Lin Htet, Feoktistov SI. *Determination of Relative Strain Corresponding to the Beginning of Neck Formation When Testing Aluminum Alloys for Rapture*. In: Proc. V All-Russian National Sci. Conf. of young scientists. Komsomolsk-on-Amur; 2022. P. 157–160.

About the Authors:

Sergey I Feoktistov, professor of the Aircraft Engineering Department, Komsomolsk-na-Amure State University (27, Lenin Prospect, Komsomolsk-on-Amur, 681013, RF), Dr.Sci. (Eng.), ResearcherID, ORCID, serg_feo@mail.ru

Ivan K Andrianov, associate professor of the Aircraft Engineering Department, Komsomolsk-na-Amure State University (27, Lenin Prospect, Komsomolsk-on-Amur, 681013, RF), Cand.Sci. (Eng.), ScopusID, ORCID, ivan_andrianov_90@mail.ru

Claimed contributorship:

SI Feoktistov: description of the theoretical part of the study of limit deformation diagrams based on the Hill-Swift criteria. IK Andrianov: calculation of the construction of limit strain curves for aviation alloys; layout of the scientific paper.

Received 13.12.2022.
Revised 09.01.2023.
Accepted 09.01.2023.

Conflict of interest statement

The authors do not have any conflict of interest.

All authors have read and approved the final manuscript.

Об авторах:

Сергей Иванович Феоктистов, профессор кафедры «Авиастроение» Комсомольского-на-Амуре государственного университета (681013, РФ, г. Комсомольск-на-Амуре, пр. Ленина, 27), доктор технических наук, ResearcherID, ORCID, serg_feo@mail.ru

Иван Константинович Андрианов, доцент кафедры «Авиастроение» Комсомольского-на-Амуре государственного университета (681013, РФ, г. Комсомольск-на-Амуре, пр. Ленина, 27), кандидат технических наук, ScopusID, ORCID, ivan_andrianov_90@mail.ru

Заявленный вклад соавторов:

С.И. Феоктистов — описание теоретической части исследования диаграмм предельного деформирования на основании критериев Хилла-Свифта. И.К. Андрианов — проведение расчета построения кривых предельных деформаций для авиационных сплавов, оформление научной статьи.

Поступила в редакцию 13.12.2022.
Поступила после рецензирования 09.01.2023.
Принята к публикации 09.01.2023.

Конфликт интересов

Авторы заявляют об отсутствии конфликта интересов.

Все авторы прочитали и одобрили окончательный вариант рукописи.